Bandgap Modulation in Efficient n-Thiophene Absorbers for Dye Solar Cell Sensitization

Eva Mª Barea,[a] Rubén Caballero,[b] Francisco Fabregat-Santiago,[a] Pilar de la Cruz,[b] Fernando Langa,[b] and Juan Bisquert*[a]

Five new sensitizers for dye sensitized solar cells have been designed consisting of conjugated thienylvinylene units threaded with alkyl chains to improve solubility and cyanoacetic acid as anchoring group. The conjugation length was increased from 2 to 6 thienylvinylene units, which resulted in a red-shift of the optical absorption of the dyes from 550 to 750 nm, improving the spectral overlap with the solar spectrum. The photovoltaic performance of these dyes as sensitizers in mesoporous TiO$_2$ solar cells shows a clear correlation of increasing photocurrent with the extension of the conjugation up to an optimal length. Further extension of the conjugation increases the absorption but additional effects like self-quenching or recombination processes reduce the photocurrent and photovoltages and consequently the overall efficiency of the DSC.

1. Introduction

Nanocrystalline semiconductor-based dye-sensitized solar cells (DSC) have attracted significant attention as low cost alternatives to conventional solid-state photovoltaic devices.[1] The most successful charge-transfer sensitizers employed so far in these cells are polypyridyl-type complexes of ruthenium[2,3] yielding overall AM 1.5 solar to electric power conversion efficiencies up to 11.3%.[4,5] But the high cost of ruthenium, the necessity of purification treatments and the low molar extinction coefficients, pose difficulties for commercial large DSC modules, hence the increasing interest of research on metal-free organic dyes.[6–8]

Organic sensitizers have the advantage of high extinction coefficients and can thus also meet the demand of good light harvesting efficiency with thinner TiO$_2$ films. New less volatile redox systems such as ionic liquids[9–12] and hole conductors[13–15] require thinner TiO$_2$ films because of mass transport limitations or insufficient pore filling. A great variety of organic sensitizers based on polyene-triphenylamine,[8,16–21] coumarin[22–24] and indoline[25–28] moieties give respectable conversion efficiencies of 5–9%[29] with the traditional iodide/triiodide redox system. Despite the promising results obtained so far, more research is needed to understand the energetic, kinetic and geometric interplay between dye, TiO$_2$ and electrolyte, to design an efficient and stable organic dye for large scale applications.

Here we present the synthesis and solar cell performance of a series of D-π-A chromophores with prolongation of π conjugation length of n oligothienylvinylene units to increase the spectral response (Figure 1). The donor unit is an oligomer of thienylvinylene with different lengths and the acceptor is the cyanoacetic acid moiety. The
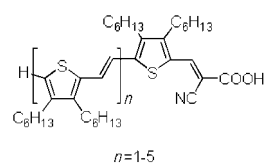
Figure 1. FLn dyes structures, n is the number of thienylvinylene units.

risk of decreased electron injection by π-stacked dye aggregation is prevented with attached alkyl groups[30] to avoid the strong π–π interaction.[31] The dyes will be denoted FLn (n = 2, 3, 4, 5 and 6, n means the number of oligothienylvinylene units) in which FL4 is the compound named RC4-17 in previous work.[32]

Experimental Section

Synthesis: The general procedure for the synthesis of the FLn dyes from thienylvinylenes (TV) is described in Figure 2 and in the Supporting Information. Under Ar, over a stirred solution of the corresponding aldehyde and cyanoacetic acid in CHCl$_3$, 2 drops of piperidine are added and the mixture is refluxed for the indicated time. The solvent is evaporated under reduced pressure and the
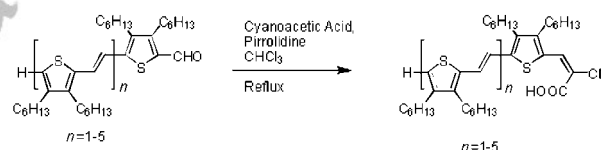
Figure 2. General synthesis of FLn dyes.

[a] Dr. E. M. Barea, Dr. F. Fabregat-Santiago, Prof. J. Bisquert
Photovoltaic and Optoelectronic Devices Group
Physics Department, Universitat Jaume I, 12071 Castelló (Spain)
Fax: (+34) 964 729218
bisquert@fca.uji.es

[b] R. Caballero, Dr. P. d. l. Cruz, Prof. F. Langa
Instituto de Nanociencia, Nanotecnología y Materiales Moleculares (INAMOL)
Universidad de Castilla La Mancha, Campus de la Antigua Fábrica de Armas
Avda. Carlos III, s/n 45071. Toledo (Spain)

Supporting information for this article is available on the WWW under http://dx.doi.org/10.1002/cphc.200900605.

These are not the final page numbers! ↗↗

obtained product is purified by column chromatography (silicagel, CHCl$_3$:MeOH 9:1).

FL2: From 2TV-CHO (153 mg, 0.27 mmol), cyanoacetic acid (35 mg, 0.41 mmol), 15 mL of CHCl$_3$. Reaction time: 22 h. Yield: 62% (106 mg, 0.17 mmol). FT–IR v/cm^{-1}: 2953, 2924, 2854, 1691, 1556, 1691, 1556, 1462, 1423, 1400, 1342, 1248, 1084, 926, 721; ^{1}H NMR (400 MHz, CD$_2$Cl$_2$) δ/ppm: 8.43 (s, 1H), 7.34 (d, ^3J=15.3 Hz, 1H), 7.04 (d, ^3J=15.3 Hz, 1H), 6.92 (s, 1H), 2.74 (m, 2H), 2.64 (m, 4H), 2.51 (t, ^3J=7.6 Hz, 2H), 1.62 (m, 2H), 1.52 (m, 6H), 1.46–1.19 (m, 24H), 0.90 (m, 12H); ^{13}C NMR (100 MHz, CDCl$_3$) δ/ppm: 168.8, 156.1, 149.1, 145.1, 144.0, 143.3, 141.1, 136.1, 128.3, 125.8, 120.5, 117.7, 116.4, 93.5, 32.1, 31.7, 31.6, 31.5, 31.4, 31.2, 30.9, 29.7, 29.6, 29.5, 29.3, 29.2, 28.9, 27.7, 27.1, 26.8, 22.6, 22.6, 22.5, 14.1, 14.0, 13.9; UV-Vis (CH$_2$Cl$_2$) λ_{max}/nm (log ε): 244.5 (4.29), 316.5 (4.36), 480.5 (4.41); EM (m/z) (MALDI-TOF) calculated for C$_{38}$H$_{57}$NO$_2$S$_2$: 623.38; found: 623.86 (M+H).

FL3: From 3TV-CHO (150 mg, 0.18 mmol), cyanoacetic acid (23 mg, 0.27 mmol), 15 mL of CHCl$_3$. Reaction time: 22 h. Yield: 89% (145 mg, 0.16 mmol). FT–IR v/cm^{-1}: 2958, 2921, 2848, 1683, 1548, 1454, 1421, 1389, 1239, 1160, 1078, 915, 915, 715; ^{1}H NMR (400 MHz, CD$_2$Cl$_2$) δ/ppm: 8.44 (s, 1H), 7.34 (d, ^3J=15.1 Hz, 1H), 7.14–7.68 (m, 3H), 6.84 (s, 1H), 2.78 (m, 2H), 2.67 (m. 8H), 2.53 (t, ^3J=7.3 Hz, 2H), 1.65 (m, 2H), 1.54 (m, 10H), 1.49–1.20 (m, 36H), 0.93 (m, 18H); ^{13}C NMR (100 MHz, CDCl$_3$) δ/ppm: 156.1, 145.0, 144.9, 143.5, 141.8, 141.1, 140.7, 137.7, 136.8, 133.9, 128.4, 125.2, 125.1, 121.2, 118.9, 118.6, 117.6, 37.1, 31.7, 31.6, 31.5, 31.4, 31.2, 31.0, 30.9, 29.7, 29.6, 29.4, 29.3, 29.2, 29.1, 27.7, 27.2, 27.0, 26.9, 26.8, 22.6, 22.5, 22.5, 14.2, 14.1, 14.0, 14.0; UV-Vis (CH$_2$Cl$_2$), λ_{max}/nm (log ε): 304.0 (4.37), 375.0 (4.19), 535.0 (4.50); EM (m/z) (MALDI-TOF) calculated for C$_{56}$H$_{85}$NO$_2$S$_3$: 899.57; found: 900.68 (M+H).

FL4: From 4TV-CHO[32]

FL5: From 5TV-CHO (75 mg, 0.05 mmol), cyanoacetic acid (7 mg, 0.08 mmol), 18 mL of CHCl$_3$. Reaction time: 20 h Yield: 66% (52 mg, 0.04 mmol). FT–IR v/cm^{-1}: 2950, 2917, 2844, 1683, 1573, 1466, 1381, 1245, 1160, 1111, 1086, 923, 792, 719; ^{1}H NMR (400 MHz, CD$_2$Cl$_2$) δ/ppm: 8.43 (s, 1H), 7.34 (d, ^3J=15.3 Hz, 1H), 7.10 (d, ^3J=15.3 Hz, 1H), 7.03 (bs, 6H), 6.81 (s, 1H), 2.78 (m, 2H), 2.64 (bs, 14H), 2.52 (m, 4H), 1.70–1.03 (m, 80H), 0.95 (m, 30H); ^{13}C NMR (100 MHz, CDCl$_3$) δ/ppm: 154.4, 155.5, 148.6, 144.9, 144.3, 143.9, 142.3, 142.0, 141.8, 141.6, 141.4, 141.0, 140.0, 137.8, 137.1, 138.9, 135.2, 134.2, 134.9, 124.2, 124.5, 124.9, 120.6, 120.0, 119.8, 119.2, 119.0, 118.0, 117.8, 116.9, 37.1, 32.8, 32.2, 32.0, 31.9, 31.7, 31.6, 31.5, 31.4, 31.2, 31.1, 31.1, 30.9, 30.0, 29.7, 29.4, 29.3, 29.0, 27.7, 27.2, 26.9, 26.8, 22.6, 14.1, 14.0; UV-Vis (CH$_2$Cl$_2$) λ_{max}/nm (log ε): 265 (4.44), 294.0 (4.58), 394.0(4.17), 578.0 (4.76); EM (m/z) (MALDI-TOF) calculated for C$_{92}$H$_{141}$NO$_2$S$_5$: 1451.95; found: 1453.28 (M+H).

FL6: From 6TV-CHO (58 mg, 0.04 mmol), cyanoacetic acid (45 mg, 0.05 mmol), 20 mL of CHCl$_3$. Reaction time: 20 h. Yield: 89% yield (56 mg, 0.03 mmol). FT–IR v/cm^{-1}: 2950, 2921, 2852, 1683, 1560, 1466, 1413, 1377, 1246, 1168, 1131, 1086, 919, 719; ^{1}H NMR (400 MHz, CD$_2$Cl$_2$) δ/ppm: 8.42 (s, 1H), 7.33 (d, ^3J=15.9 Hz, 1H), 7.10 (d, ^3J=15.9 Hz, 1H), 7.03 (bs, 8H), 6.81 (s, 1H), 2.78 (m, 2H), 2.64 (m, 18H), 2.52 (t, ^3J=7.3 Hz, 4H), 1.70–1.20 (m, 96H), 0.95 (m, 36H); ^{13}C NMR (100 MHz, CDCl$_3$) δ/ppm: 145.0, 143.4, 142.4, 142.0, 141.9, 141.7, 141.6, 141.4, 141.0, 141.0, 137.9, 137.2, 137.1, 136.0, 135.9, 135.5, 135.2, 135.1, 134.9, 134.2, 128.6, 125.6, 125.0, 124.9, 120.7, 119.9, 119.9, 119.8, 119.6, 119.3, 119.2, 119.0, 117.9, 32.0, 31.7, 31.6, 31.5, 31.2, 30.9, 29.7, 29.4, 29.3, 29.0, 27.0, 22.7, 22.6, 14.1, 14.0; UV/Vis (CH$_2$Cl$_2$), λ_{max}/nm (log ε): 292.5 (4.45), 367.0 (3.88), 435.0 (4.11), 583.0 (4.67); EM (m/z) (MALDI–TOF) calculated for C$_{110}$H$_{169}$NO$_2$S$_6$: 1728.14; found: 1730.56 (M+2H).

Dye Sensitized Solar Cells: Dye solar cells (DSC) were prepared using TiO$_2$ nanocrystalline paste prepared by hydrolysis of titanium tetraisopropoxide[1] with the addition of ethyl cellulose as binder in α-terpineol. The TiO$_2$ layers were deposited using the doctor blading technique on transparent conducting oxide (TCO) glass (Pilkington TEC15, ~15 Ω/sq resistance). The resulting photoelectrodes of 10 µm thickness, were sintered at 450 °C and then immersed in 0.04 M TiCl$_4$ solution for 30 min at 70 °C followed by calcination at 450 °C for 30 min. When the temperature decreased until 40 °C all the electrodes were immersed into dye solution (0.3 mM in dichloromethane) overnight (16 h). After the adsorption of the dye, the electrodes were rinsed with the same solvent. The solar cells were assembled with the counter electrode (thermally platinized TCO) using a thermoplastic frame (Surlyn 25 µm thick). Redox electrolyte [0.5 M LiI (99,9%) and 0.05 M I$_2$ (99,9%) in 15/85 (v/v) mixture of Valeronitrile and Acetonitrile] was introduced though a hole drilled in the counter electrode that was sealed afterwards. Prepared solar cells (with 0.5 cm^2 active area and a mask of 0.35 cm^2) were characterized by current–voltage characteristics, IPCE and impedance spectroscopy. Photocurrent and voltage were measured using a solar simulator equipped with a 1000W ozone-free Xenon lamp and AM 1.5 G filter (Oriel), were the light intensity was adjusted with an NREL-calibrated Si solar cell with a KG-5 filter to 1 sun light intensity (100 mWcm^{-2}).

2. Results and Discussion

The normalized UV/Vis absorbance spectra of the dyes in dichloromethane (DCM) and absorbed onto 4 µm thick nanocrystalline TiO$_2$ films (Figure 3) present a systematic red-shift in the absorption maximum with increasing conjugation. Upon the absorption onto
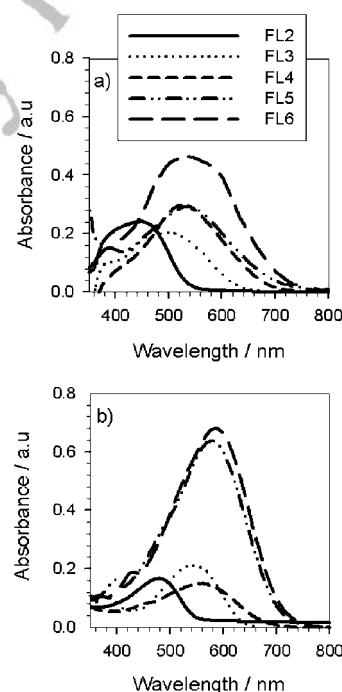
Figure 3. a) Normalized absorption spectra of FL*n* dyes anchored in the transparent nanocrystalline titania film. The absorption from the titania and glass substrate has been subtracted. b) UV/Vis spectra of FL*n* dyes in dichloromethane.

↖↖ These are not the final page numbers!

TiO$_2$ the dye spectra are broadened. It is well established in the literature[33] that push–pull chromophores based on thienylvinylene present intense solvatochromism, hence the absorption bands can shift in wavelength due to the different solvent polarity. This effect has been checked dissolving FL4 in butanol and DCM. In this case the solvent effect causes a slight shift of the maximum, from 531 nm for butanol to 557 nm for DCM (data not shown).

It is found that the HOMO level (vs NHE) rises with the increasing length (*n*) of the thiophene chain, but it remains at potentials more positive than the iodine/iodide redox potential value (Table 1), indicating that the regeneration of the oxidized dyes

Table 1. Experimental spectral and electrochemical properties of the dyes.

Dye	Abs$_{max}$ [nm][a]	ε [M^{-1} cm^1]	$E_{(S+/S)}$ [V] vs NHE[b]	$E_{(0-0)}$ [V][c]	$E_{(S+/S^*)}$ [V] vs NHE[d]
FL2	480	25.979	1.42	1.98	−0.56
FL3	535	31.966	0.96	1.71	−0.75
FL4	557	12.807	0.80	1.60	−0.80
FL5	578	57.955	0.80	1.50	−0.70
FL6	583	47.053	0.72	1.45	−0.73

[a] Absorption spectra of dyes in DCM solution, [b] the ground state oxidation potential of the dyes was measured with DPV under the following conditions: Pt working electrode and Pt counterelectrode, electrolyte, 0.1 M tetrabutylammonium hexafluorophosphate, TBA(PF6), in dichloromethane. Potentials measured vs Ag/AgCl were converted to normal hydrogen electrode (NHE) by addition of +0.22 V, [c] 0–0 transition energy, $E_{(0-0)}$, estimated from the intercept of the normalized absorption and emission spectra in DCM, [d] Estimated LUMO energies, E$_{(LUMO)}$ vs NHE from the estimated highest occupied molecular orbital (HOMO) energies obtained from the ground state oxidation potential by adding the 0–0 transition energy, $E_{(0-0)}$.

with I$^-$ ions is thermodynamically possible. The LUMO level in the case of 2FL (−0.56 V vs NHE) is slightly more negative than the conduction band energy of TiO$_2$ (E_C) for acid TiO$_2$ paste (~ −0.5 V vs NHE). The LUMO level increases slightly when *n* increases, therefore, these types of sensitizers have sufficient driving force for electron injection to TiO$_2$.

Using density functional theory (DFT) at the B3LYP/6-31G (Figure 4) it is observed that the HOMO is distributed along the conjugated system and the LUMO is located over the cyanoacetic unit through thiophene allowing significant charge separation within the dye after photo-excitation. Furthermore the location of the LUMO at the side of the TiO$_2$ surface and the HOMO at the opposite end of the molecule, eases the electron injection into the semiconductor
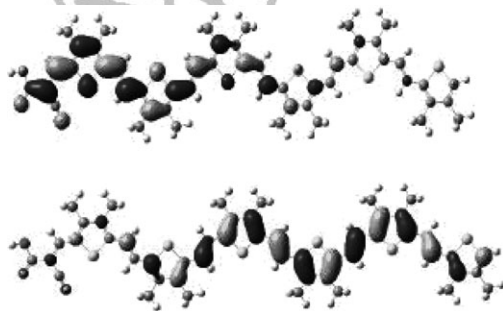
Figure 4. Frontier orbitals LUMO (top) and HOMO (bottom) of FL6 dye optimized at the B3LYP/6-31G level.

and prevents back regeneration of the dye with the injected electrons. The distribution of the HOMO along the whole conjugated chain also improves the regeneration of the dyes with the redox couple. Efficient photoinduced electron transfer from FL*n* to good electron acceptors as C$_{60}$ has been previously observed.[34, 35]

In good agreement with the absorption spectra of Figure 3, the incident photon-to-current conversion efficiency (IPCE) of the sensitizers in Figure 5, increases and broadens as the conjugation
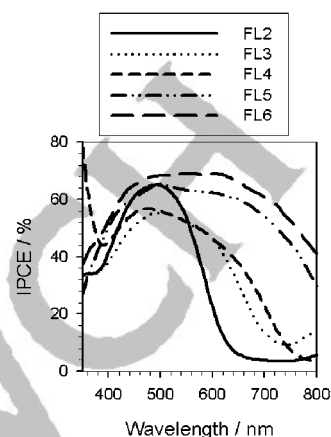
Figure 5. IPCE spectra for DSCs based on oligothienylvinylene sensitizers.

length (*n*) rises. FL2 exhibits a localized maximum of 65% but the spectrum is narrow, resulting in lower overall efficiencies due to spectral limitations. FL3 and FL4 show a broad IPCE with a maximum around 55%, giving an increase in the overall efficiencies of DSC based on FL3 and FL4 dyes. Solar cells based on FL5 and FL6 show even broader IPCE in accordance to the broad absorption spectrum achieved by increasing the linker conjugation. In the IPCE, the broadening of the absorption spectra is remarkable, yielding an extension in the absorption to ≈100 nm higher wavelengths. This absorption at lower wavelengths is due both to the use of thicker and scattering TiO$_2$ films and to the interaction between the absorbed dye and the electrolyte mentioned above.

The photovoltaic performance of solar cells based on FL2, FL3, FL4, FL5 and FL6 dyes under AM 1.5G illumination (100 mW cm^{-2}), is summarized in Table 2 and light current-voltage curves are shown in Figure 6. The electrolyte composition is 0.5 M LiI (99.9%) and 0.05 M I$_2$ (99.9%) in 15/85 (v/v) mixture of valeronitrile and acetonitrile. No more additives to the electrolyte were added due to the fact that the conduction band of the TiO$_2$ must be kept down inasmuch as is possible, taking into account the energies of the semiconductor and the dyes (see Table 1). Otherwise, injection from the excited dye to the conduction band of the TiO$_2$ can be inhibited.[32] In order to avoid possible aggregation phenomena that could

Table 2. Photovoltaic performance of FL*n* family dyes.

Dye	J_{sc}[mA cm^{-2}][a]	V_{oc} [V][b]	FF[c]	η [%][d]
FL2	8.49	0.33	0.51	1.43
FL3	12.4	0.41	0.52	2.67
FL4	13.4	0.50	0.57	3.84
FL5	15.8	0.44	0.38	2.68
FL6	13.2	0.37	0.37	1.80

[a] Short circuit photocurrent density, [b] Open circuit potential voltage, [c] Fill factor, [d] Power conversion efficiency

These are not the final page numbers! ↗↗
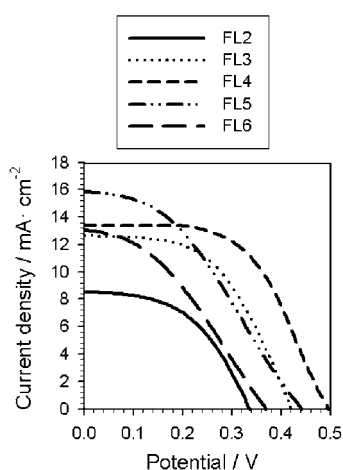
Figure 6. Current density–potential curves for DSCs at 1 sun with FL*n* as sensitizers.

appear with the length of the dye molecule, DSCs were prepared using chenodeoxycholic acid (DCA) as a co-adsorbent obtaining the same values of j_{sc}. This confirms that the design of the dyes prevents π-stacked aggregation (Figure 7). Measurements of the *j–V* curve were done one week later to check the stability of the dye and the results were the same.
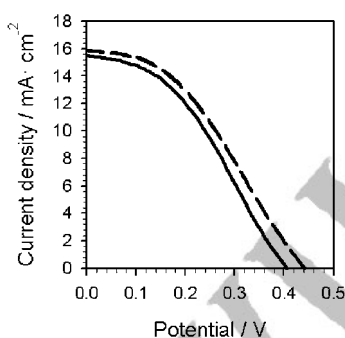
Figure 7. Current density-potential curves at 1 sun obtained with FL5 as sensitizer, coabsorbed with (line) and without chenodeoxycholic acid (dash).

The efficiency obtained with FL*n* dyes is increasing with the number of TV units, from FL2 to FL4 (see Table 2), but when the molecule dye is longer (FL5 and FL6), although the light harvesting is enhanced, the efficiency drops down. It has been reported in the literarure that several factors could cause such a decrease, like the internal difference in dye load. Assuming a monolayer of the adsorbed dye onto TiO$_2$, a larger dye will have a larger footprint (excluded volume) and hence result in lower dye load, that in conjunction with binding and orientation problems, could affect the injection efficiency.[8] But the most important factors observed in Table 2 for FL4 and higher are: i) the photocurrent at short circuit is not increasing as expected, ii) a fall in the open-circuit voltage (V_{oc}) and iii) an important decrease of the fill factor (FF),[36] when the length of the dye molecule increases.

Since all the conditions of the solar cells are similar, one expects from the higher IPCE and absorbance of F5 and FL6 that these dyes will produce the highest photocurrents, and this is not the case for FL6. Furthermore, a decrease in efficiency is already observed for FL5 that is more pronounced for FL6. One conjectures

that the origin of the lowered efficiency, the drop in FF and the decrease of the V_{oc} for FL5 and FL6, must be related to an increased recombination rate in the presence of the longer chain dyes. Intuitively, one expects recombination to govern the *j–V* curve behaviour close to V_{oc}, and not at low voltages. But it is appreciated in Figure 6 that FL2, FL3 and FL4 solar cells, all trace a plateau of the current, which indicates a saturation of photocurrent in the extraction regime of the solar cell, while this does not occur for FL5 and FL6. This means that recombination is controlling these last two solar cells *even at low voltage*, and not all the electrons photoinjected in the TiO$_2$ can be extracted. It should be recalled that IPCE current is measured at very low electron density, in which condition recombination rate should be considerably lower than at 1 sun. It is also possible that since the bandgap is shrinking at high *n* in FL*n*, and the HOMO level becomes slightly less positive, the driving force for regeneration of the oxidized dye approaches the regeneration threshold at these high intensities (recall that this is not observed the low intensity measurement of IPCE), thus reducing the photocurrent.

In order to clarify these assumptions, impedance spectroscopy (IS) measurements were performed on the cells (FL2, FL3, FL5 and FL6). All measurements were carried out under an irradiation of 1 sun at AM 1.5 conditions, and different bias potentials that ranged from 0 to 0.45 V and frequencies between 1 MHz and 0.1 Hz. These measurements were analyzed using the impedance model developed by Bisquert et al.,[37–39] that allows to isolate the recombination resistance (which is related to recombination flux[40]) from other resistive contributions in the cell. The recombination resistance evaluated from IS, shown in Figure 8, clearly indicates differ-
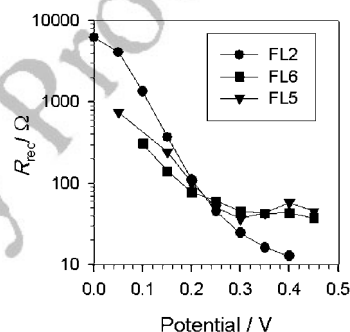
Figure 8. Charge-transfer resistance versus applied potential.

ences in the charge recombination kinetics of the cells. In the case of FL2 and FL3 (not shown since it presents very close values of R_{rec} to FL2), the slope of R_{rec} vs the potential is much higher than the slopes of samples FL5 and FL6. The consequence of these changes is the important reduction in the FF[38] observed in Table 2. Furthermore, for the *lower* values of the potential, the R_{rec} is higher for FL2 (and FL3), which means that at the same Fermi level, the DSCs with FL5 and FL6 present larger recombination losses from the TiO$_2$ towards the redox couple than sample with FL2. As a consequence, the bending of the plateau of the *j–V* curve towards the V_{oc} occurs at lower potentials and this produces a decrease of V_{oc}. This is the case of FL6, which in spite of having a similar short circuit current (charge collection) to FL3, the photopotential is reduced to a value very close to the FL2 sample. In the case of FL5, the V_{oc} obtained is enhanced, with respect to FL6 by the larger number of electrons collected by the cell, that displaces upwards the *j–V* curve of FL6 to match the one from FL5 but, again, the V_{oc} is very close to FL3 with much less short circuit cur-

↖↖ These are not the final page numbers!

rent. Part of the difference between the short circuit current density of FL5 and FL6 could be in the smaller R_{rec} value that can be observed in Figure 8 for the lowest potentials. It cannot be excluded that at high illumination intensity the current is also partly limited by the decreased regeneration rate of the dyes absorbed in the TiO_2 surface.

In summary the impedance results therefore confirm that the decreasing efficiency at high number of TV units in the FL*n* dyes, despite the higher photon collection, is due to an increased recombination rate, which impedes charge extraction, even at voltages close to short-circuit condition. The mechanistic origin of the increased recombination should be further investigated.

3. Conclusions

A family of organic dyes based on oligothienylvinylene units showing high absorption in the visible and NIR region have been synthesised and their application in dye solar cells studied. The dyes do not present any aggregation phenomena. By increasing the π-conjugation of the *n*TV, the HOMO and LUMO energy levels were modified. Calculations show that LUMO is distributed over the *n*TV units and the HOMO over the cyanoacetic acid. Dyes FL2, FL3 and FL4 give reasonable efficiencies, increasing with the number of *n*TV units. For the longers dyes, FL5 and FL6, despite the broader spectral response, the solar cells present an increase in the recombination of electrons to the triiodide, decreasing dramatically the V_{oc} and in consequence the efficiency. The FL*n* family of dyes appears suitable for their use not only for DSC with liquid electrolyte, but also for future solid state applications due to the high extinction coefficient that they present.

[1] B. O'Regan, M. Grätzel, *Nature* **1991**, *353*, 737.

[2] A. Kay. M. K. Nazeeruddin, I. Rodicio, R. Humphry - Baker, E. Muller, P. Linska, N. Vlachopoulous and M. Grätzel, *J. Am. Chem. Soc.* **1993**, *115*, 6382–6390.

[3] F. P. Rotzinger, P. Pechy, M. K. Nazeeruddin, O. Kohle, S. M. Zakeeruddin, R. Humphry - Baker and M. Grätzel, *J. Am. Chem. Soc.* **1995**, *117*■■*ok?*■■*65*.

[4] F. Gao, Y. Wang, D. Shi, J. Zhang, M. Wang, X. Jing, R. Humphry-Baker, P. Wang, S. M. Zakeeruddin, M. Gratzel, *J. Am. Chem. Soc.* **2008**, *130*, 10720–10728.

[5] A. Islam, Y. Chiba, Y. Watanabe, R. Kominaya, N. Koide and L. Han, *Jpn. J. Appl. Phys. Part 2* **2006**, *45*, L638.

[6] S. Kim, J. K. Lee, S. O. Kang, J. Ko, J. H. Yum, S. Fantacci, F. De Angelis, D. Di Censo, M. K. Nazeeruddin and M. Grätzel, *J. Am. Chem. Soc.* **2006**, *128*, 16701–16707.

[7] W. Xu, M. Liang, F. Cai, P. Chen, B. Peng, J. Chen and Z. Li, *J. Phys. Chem. A J. Phys. Chem. C* **2007**, *111*, 4465–4472.

[8] T. Marinado, D. P. Hagberg, K. M. Karlsson, K. Nonomura, P. Qin, G. Boschloo, T. Brinck, A. Hagfeldt and L. Sun, *J. Org. Chem.* **2007**, *72*, 9550.

[9] S. M. Zakeeruddin, S. Ito, R. Humphry-Baker, P. Liska, R. Charvet, P. Comte, M. K. Nazeeruddin, M. Péchy, M. Takata, H. Miura, S. Uchida, M. Grätzel, Adv. Mater. **2006**, *18*, 1202–1205.

[10] N. Papageorgiou, Y. Athanassov, M. Armand, P. Bonhote, H. Pettersson, A. Azam, M. Gratzel, *J. Electrochem. Soc.* **1996**, *143*, 3099–3108.

[11] S. M. Zakeeruddin, P. Wang, M. Grätzel, W. Kantlehner, J. Mezger, E. V. Stoyanov and O. Scherr, *Appl. Phys. A*■■ok?■■ **2004**, *79*, 73–77.

[12] P. Wang, S. M. Zakeeruddin, J.-E. Moser, R. Humphry-Baker, M. Gratzel, *J. Am. Chem. Soc.* **2004**, *126*, 7164–7165.

[13] L. Schmidt-Mende, U. Bach, R. Humphry-Baker, T. Horiuchi, H. Miura, S. Ito, S. Uchida, M. Grätzel, *Adv. Mater.* **2005**, *17*, 813–815.

[14] D. Lupo, U. Bach, P. Comte, J. E. Moser, F. Weissortel, J. Salbeck, H. Spreitzer, M. Gratzel, *Nature* **1998**, *395*, 583–585.

[15] J. Hagen, W. Schaffrath, P. Otschik, R. Fink, A. Bacher, H.-W. Schmidt, D. Haarer, *Syn. Metals.* ■■ok?■■ **1997**, *89*, 215–220.

[16] S. Kim, J. K. Lee, S. O. Kang, J. Ko, J. H. Yum, S. Fantacci, F. De Angelis, D. Di Censo, M. K. Nazeeruddin, M. Gratzel, *J. Am. Chem. Soc.* **2006**, *128*, 16701–16707.

[17] T. Edvinsson, Daniel P. Hagberg, T. Marinado, G. Boschloo, A. Hagfeldt and L. Sun, *Chem. Commun.* **2006**, *21*, 2245–2247.

[18] K. Hara, T. Sato, R. Katoh, A. Furube, T. Yoshihara, M. Murai, M. Kurashige, S. Ito, A. Shinpo, S. Suga, H. Arakawa, *Adv. Funct. Mater.* **2005**, *15*, 246–252.

[19] T. Kitamura, M. Ikeda, K. Shigaki, T. Inoue, N. A. Anderson, X. Ai, T. Lian, S. Yanagida, *Chem. Mater.* **2004**, *16*, 1806–1812.

[20] D. P. Hagberg, J.-H. Yum, H. Lee, F. De Angelis, T. Marinado, K. M. Karlsson, R. Humphry-Baker, L. Sun, A. Hagfeldt, M. Grätzel, M. K. Nazeeruddin, *J. Am. Chem. Soc.* **2008**, *130*, 6259–6266.

[21] H. Qin, S. Wenger, M. Xu, F. Gao, X. Jing, P. Wang, S. M. Zakeeruddin, M. Gratzel, *J. Am. Chem. Soc.* **2008**, *130*, 9202–9203.

[22] K. Hara, Z.-S. Wang, T. Sato, A. Furube, R. Katoh, H. Sugihara, Y. Dan-oh, C. Kasada, A. Shinpo, S. Suga, *J. Phys. Chem. B* **2005**, *109*, 15476–15482.

[23] K. Hara, T. Sato, R. Katoh, A. Furube, Y. Ohga, A. Shinpo, S. Suga, K. Sayama, H. Sugihara, and H. Arakawa, J. Phys. Chem. B. **2003**, *107*, 597.

[24] K. Samaya, K. Hara, H. Arakawa, Y. Ohga, A. Shinpo and S. Suga, *Chem. Commun.* **2001**, *6*, 569–570.

[25] H. Miura, T. Horiuchi, and S. Uchida, *Chem. Commun.* **2003**, 3036–3037.

[26] T. Horiuchi, H. Miura, K. Sumioka, S. Uchida, *J. Am. Chem. Soc.* **2004**, *126*, 12218–12219.

[27] T. Horiuchi, H. Miura, S. Uchida, *J. Photochem. Photobiol. A* **2004**, *164*, 29–32.

[28] K. Daibin, U. Satoshi, H.-B. Robin, M. Z. Shaik , G. Michael, *Angew. Chem.* **2008**, *120*, 1949–1953; *Angew. Chem. Int. Ed.* **2008**, *47*, 1923–1927.

[29] J. Ho Lee. S. Hwang, C. Park, H. Lee, C. Kim, Chiyoung Park, Mi-Hyeon Lee, W. Lee, J. Park, K. Kim, N-G. Park and Ch. Kim, *Chem. Commun.* **2007**, 4887–4889.

[30] N. Koumura, Z. S. Wang, S. Mori, M. Miyashita, E. Suzuki, K. Hara, *J. Am. Chem. Soc.* **2006**, *128*, 14256–14257.

[31] P. Pechy, T. Renouard, S. M. Zakeeruddin, R. Humphry-Baker, P. Comte, P. Liska, L. Cevey, E. Costa, V. Shklover, L. Spiccia, G. B. Deacon, C. A. Bignozzi, M. Gratzel, *J. Am. Chem. Soc.* **2001**, *123*, 1613–1624.

[32] R. Caballero, E. M. Barea, F. Fabregat-Santiago, P. de La Cruz, L. Márquez, F. Langa, J. Bisquert. *J. Phys. Chem. C.* **2008**, *112*, 18623–18627.

[33] H. Ruiz Delgado, V. Casado, J.; López Navarrete, J. T.; Raimundo, J. M.; Blanchard, P.; Roncali, *Chem. Eur. J.* ■■ok?■■ **2003**, *9*, 3670–3682.

[34] Roncali, *J. Chem. Soc. Rev.* **2005**, *34*, 483–495.

[35] S. Islam, F. Oswald, Y. Araki, V. Troiani, R. Caballero, P. De La Cruz, O. Ito, F. Langa, *Chem. Commun.* **2007**, 4498–4500.

[36] V. Thavasi, V. Renugopalakrishnan, R. Jose, S. Ramakrishna, *Mater. Sci. Eng. R* **2009**, *63*, 81–99.

[37] J. Bisquert, *J. Phys. Chem. B* **2002**, *106*, 325–332.

[38] J. Bisquert, F. Fabregat-Santiago, E. Palomares, L. Otero, D. Kuang, S. M. Zakeeruddin and M. Gratzel, *J. Phys. Chem. C* **2007**, *111*, 6550–6560.

[39] S. Ito, Q. Wang, M. Grätzel, F. Fabregat-Santiago, I. Mora-Seró, J. Bisquert, G. Bossho and H. Imai, *J. Phys. Chem. B* **2006**, *110*, 19406.

[40] J. Bisquert, F. Fabregat-Santiago, I. Mora-Seró, G. Garcia-Belmonte and S. Giménez, *J. Phys. Chem. C* **2009**, DOI:10.1021/jp9037649).

These are not the final page numbers! ⤤⤤

ARTICLES

E. M. Barea, R. Caballero,
F. Fabregat-Santiago, P. d. l. Cruz,
F. Langa, J. Bisquert*

■■ – ■■

Bandgap Modulation in Efficient n-Thiophene Absorbers for Dye Solar Cell Sensitization
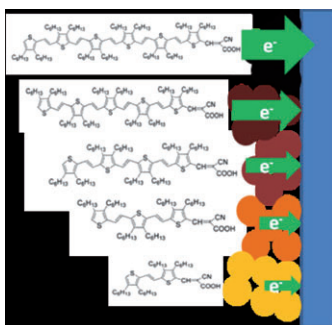
Dyes as sensitizers: Increasing the conjugation length of thienylvinylene dyes results in a red-shift of the optical absorption from 550 to 750 nm, improving the spectral overlap with the solar spectrum. The photovoltaic performance of these dyes as sensitizers in mesoporous TiO$_2$ solar cells shows a clear correlation of increasing photocurrent with the extension of the conjugation up to an optimal length (see figure).

↖↖ These are not the final page numbers!